

Geophysical Research Letters®



RESEARCH LETTER

10.1029/2024GL111078

Seabed Seismographs Reveal Duration and Structure of Longest Runout Sediment Flows on Earth

Key Points:

- Remote seismic monitoring reveals the duration, internal structure, and evolution of powerful canyon-flushing turbidity currents
- Flows contain dense and fast frontal-zones (up to ~400 km long) that maintain uniform durations and speeds despite huge seabed erosion
- Canyon-flushing flow frontal-zones can bring substantial fluxes of organic carbon, sediment, and warm water to the deep-sea in <24 hr

Supporting Information:

Supporting Information may be found in the online version of this article.









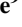





Correspondence to:

M. L. Baker,
megan.l.baker@durham.ac.uk

Citation:

Baker, M. L., Talling, P. J., Burnett, R., Pope, E. L., Ruffell, S. C., Urlaub, M., et al. (2024). Seabed seismographs reveal duration and structure of longest runout sediment flows on Earth. *Geophysical Research Letters*, 51, e2024GL111078. <https://doi.org/10.1029/2024GL111078>

Received 19 JUL 2024
Accepted 6 NOV 2024

Megan L. Baker¹ , Peter J. Talling^{1,2} , Richard Burnett³, Ed L. Pope¹ , Sean C. Ruffell² , Morelia Urlaub⁴ , Michael A. Clare⁵, Jennifer Jenkins² , Michael Dietze^{6,7} , Jeffrey Neasham³ , Ricardo Silva Jacinto⁸, Sophie Hage⁹ , Martin Hasenhüttl^{10,11} , Steve M. Simmons¹² , Catharina J. Heerema^{2,13} , Maarten S. Heijnen^{5,14}, Pascal Kunath⁴, Matthieu J. B. Cartigny¹ , Claire McGhee¹⁵, and Daniel R. Parsons¹⁶ 

¹Department of Geography, Durham University, Durham, UK, ²Department of Earth Sciences, Durham University, Durham, UK, ³School of Engineering, Newcastle University, Newcastle Upon Tyne, UK, ⁴GEOMAR Helmholtz Centre for Ocean Research, Kiel, Germany, ⁵National Oceanography Centre, Southampton, UK, ⁶Department of Geography, Georg-August-University, Göttingen, Germany, ⁷Section 4.6 Geomorphology, Deutsches GeoForschungsZentrum GFZ Potsdam, Potsdam, Germany, ⁸Geo-OceanUnit, IFREMER Centre de Brest, Plouzané, France, ⁹GEOPS, UMR 8148, Université Paris-Saclay, Orsay, France, ¹⁰Institute of Hydraulic Engineering and Water Resources Management, TU Wien, Vienna, Austria, ¹¹Institute for Hydraulic Engineering and Hydrometry, Federal Agency for Water Management, Vienna, Austria, ¹²Energy and Environment Institute, University of Hull, Hull, UK, ¹³Expert Analytics, Oslo, Norway, ¹⁴School of Ocean and Earth Sciences, University of Southampton, Southampton, UK, ¹⁵School of Natural and Environmental Sciences, Newcastle University, Newcastle, UK, ¹⁶The Loughborough Centre for Sustainable Transitions: Energy, Environment and Resilience, Loughborough University, Leicestershire, UK

Abstract Turbidity currents carve the deepest canyons on Earth, deposit its largest sediment accumulations, and break seabed telecommunication cables. Powerful canyon-flushing turbidity currents break sensors placed in their path, making them notoriously challenging to measure, and thus poorly understood. This study provides the first remote measurements of canyon-flushing flows, using ocean-bottom seismographs located outside the flow's destructive path, revolutionizing flow monitoring. We recorded the internal dynamics of the longest sediment flows yet monitored on Earth, which traveled >1,000 km down the Congo Canyon-Channel at 3.7–7.6 m s⁻¹ and lasted >3 weeks. These observations allow us to test fundamental models for turbidity current behavior and reveal that flows contain dense and fast frontal-zones up to ~400 km in length. These frontal-zones developed near-uniform durations and speeds for hundreds of kilometres despite substantial seabed erosion, enabling flows to rapidly transport prodigious volumes of organic carbon, sediment, and warm water to the deep-sea.

Plain Language Summary Seafloor avalanches of sediment, called turbidity currents, transport huge volumes of sediment and organic carbon to the deep-sea, and they break critical seabed telecommunication cables that underpin global data transfer. However, turbidity currents are very difficult to measure directly as they often damage sensors placed in their flow path, so they are poorly understood. Here we show that turbidity currents generate ground vibrations that can be measured using ocean-bottom seismographs placed outside the flow's destructive path, revolutionizing flow monitoring. These seismographs recorded the longest sediment flows yet measured in action on Earth, which traveled >1,000 km along the submarine Congo Canyon-Channel offshore West Africa. We use these observations to test fundamental models of turbidity current flow behavior. Our measurements show that the front of the flows contain a fast frontal-zone with high sediment concentrations, which can be up to ~400 km long, whilst the whole duration of the flow can last for more than 3 weeks. These frontal-zones develop near-uniform durations and speeds, despite extensive seabed erosion that adds sediment into the flow. New information on flow durations shows how turbidity currents rapidly deliver prodigious volumes of organic carbon, sediment, and warm water to the deep-ocean floor.

1. Introduction

Passive seismic monitoring has led to step changes in understanding of Earth surface processes, including globally important terrestrial geohazards such as lake outburst floods, debris flows, lahars, snow or rock avalanches, and landslides (Cook & Dietze, 2022). This method uses seismographs to remotely sense ground motions generated by hazardous events, sometimes located thousands of kilometres away, at millisecond temporal

© 2024. The Author(s).

This is an open access article under the terms of the [Creative Commons Attribution License](https://creativecommons.org/licenses/by/4.0/), which permits use, distribution and reproduction in any medium, provided the original work is properly cited.

resolution and relatively low cost. This approach has improved natural hazard detection, enabled development of life-saving early warning systems and aided effective disaster response (Luckett et al., 2007; Shugar et al., 2021). However, the potential for passive seismic monitoring of seafloor processes is only now starting to be realised (Arai et al., 2013; Clare et al., 2024; Fan et al., 2020; Gomberg et al., 2021; Sgroi et al., 2014). Indeed, seismic measurements have the potential to advance understanding of seabed dynamics even more than terrestrial processes, as seabed events are far harder to measure in action via other techniques, ensuring that there are far fewer direct observations (e.g., Talling et al., 2023).

Here, we present the first seismic observations of the longest runout sediment flows on Earth, which form many of our planet's deepest canyons and largest sediment accumulations (submarine fans). These seabed sediment-laden flows, called turbidity currents, link rivers to the deep-sea, damage critical seafloor infrastructure, transport and bury globally significant amounts of organic carbon, and can both support and destroy unique deep-sea ecosystems (Galy et al., 2007; Gavey et al., 2017; Mountjoy et al., 2018; Pope et al., 2017; Seabrook et al., 2023; Sen et al., 2017). The two turbidity currents described herein traveled for >1,000 km at speeds of 3.7–7.6 m s⁻¹ through the submarine Congo Canyon-Channel, offshore West Africa (Figure 1a). These flows broke seafloor telecommunication cables crossing the canyon multiple times during the COVID-19 pandemic, slowing internet traffic at a critical time (Talling et al., 2022).

Turbidity currents are extremely difficult to monitor in action, especially the largest and most powerful events that flush submarine canyons and runout to the deep-sea. Direct measurements of short runout (<50 km) turbidity currents have been limited to ~12 sites worldwide and were reliant on instruments placed in the flow path on anchored moorings (Azpiroz-Zabala et al., 2017; Khripounoff et al., 2003; Vangriesheim et al., 2009), which were often broken by the flows (e.g., Paull et al., 2018). Large, canyon-flushing flows have previously been measured in action at just two sites, including the Congo Canyon-Channel, but these measurements only recorded the transit speed of the flow front based on timings of broken moorings or submarine cable breaks (Carter et al., 2012; Gavey et al., 2017; Talling et al., 2022). Here, we show how powerful turbidity currents can be monitored using ocean-bottom seismographs (OBSs) located outside the flow, and thus out of harm's way. This new approach opens the way for measuring hazardous turbidity currents safely, for long deployment periods, at relatively low cost.

Preceding work has shown that the >1,000 km runout flows in the Congo Canyon-Channel eroded a globally significant mass of terrestrial organic carbon, equivalent to 22% of the annual global particulate organic carbon export from all rivers to the oceans (Baker, Hage, et al., 2024). The organic carbon showed limited degradation as it was transferred through the system, indicating efficient transport. In this study, we document the duration and internal structure (how sediment concentration and velocity change in space and time within a flow) of canyon-flushing turbidity currents for the first time, which demonstrates why the transport of terrestrial organic carbon to the deep-sea by canyon-flushing flows is efficient.

A range of models have been proposed for the flow behavior and evolution of turbidity currents, based on theory and shallow-water flow observations (e.g., Azpiroz-Zabala et al., 2017; Heerema et al., 2020; Parker, 1982; Pope et al., 2022). Appropriate models are essential for predicting flow parameters (e.g., runout distance) and the risks flows pose as geohazards. The unique observations presented here offer direct evidence to test turbidity current flow models for canyon-flushing flows.

This study has three aims: (a) demonstrate how passive seismic monitoring enables remote sensing of turbidity currents at a safe distance, including powerful canyon-flushing flows; (b) test fundamental models for how turbidity currents behave; and (c) use our unique observations of flow durations to constrain the fluxes of organic carbon, sediment, and warm water to the deep-sea by canyon-flushing turbidity currents.

2. Turbidity Currents Previously Recorded in the Congo Canyon-Channel

The Congo Canyon extends offshore from the mouth of the Congo River (Figure 1a); the second largest river in the world by discharge and fifth largest in terms of annual particulate organic carbon export (Babonneau et al., 2010; Coynel et al., 2005; Savoye et al., 2009). The first ~150 km of the canyon is deeply incised (up to 1,200 m) into the continental shelf (Figure 1b), before becoming a less incised channel on the lower slope (250–150 m deep, Figure 1c), which finally terminates 1,100 km from the river mouth at a depositional lobe. Previous work recorded turbidity currents in the upper canyon (~2,000 m water depth) for ~30% of the time during monitoring periods, using moorings with acoustic Doppler current profilers (ADCPs) that record flow velocities

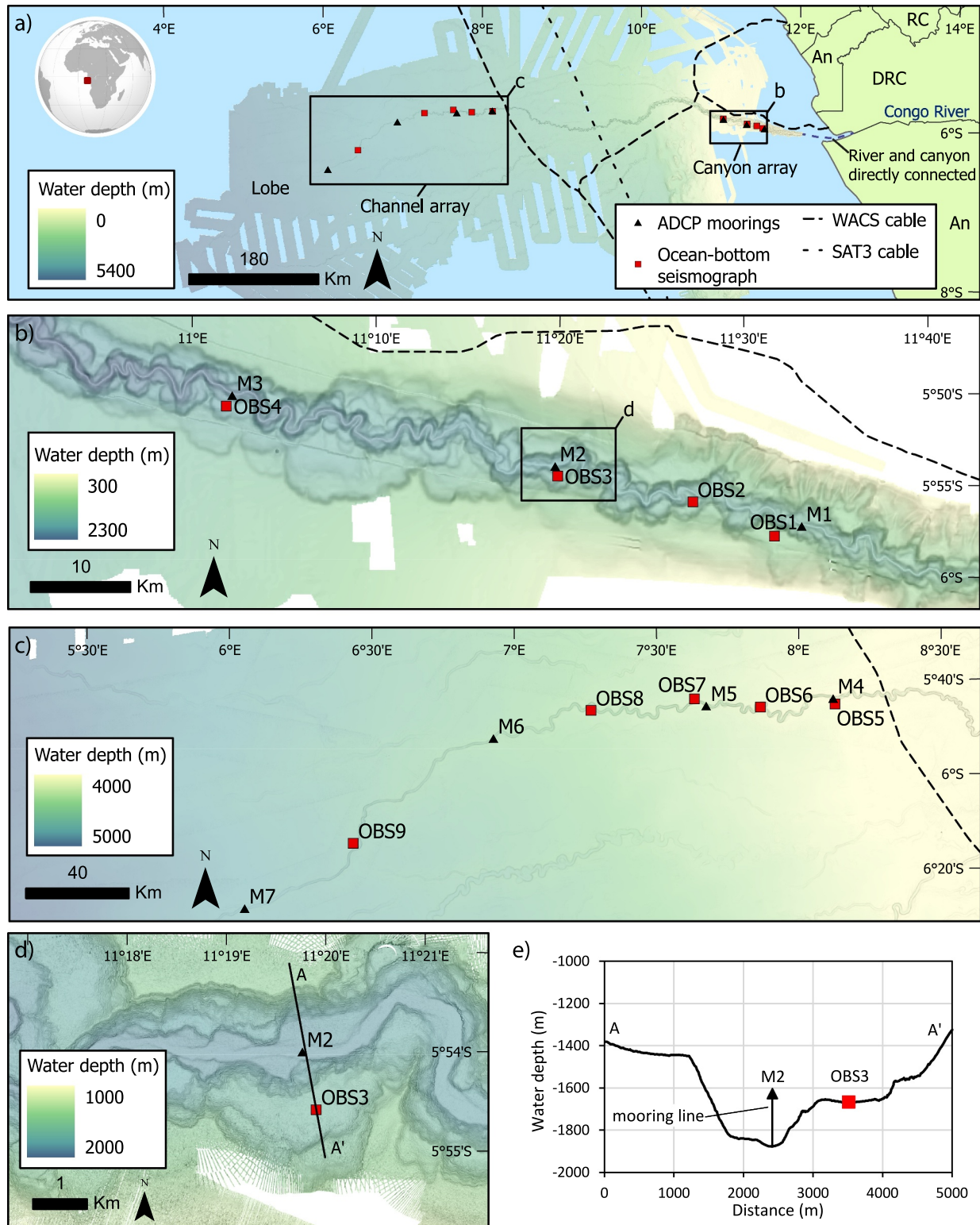


Figure 1. Instruments deployed in the Congo Canyon-Channel. (a) Bathymetric map of Congo Canyon-Channel system, offshore west Africa (location on inset world map), with instruments deployed in canyon (b) and channel (c) subarrays. (d, e) Acoustic Doppler current profiler (ADCP) moorings (black triangles) were located inside the canyon and channel, where the anchored mooring lines were broken by the first canyon-flushing turbidity current, whilst ocean-bottom seismographs (OBS; red squares) were safely located outside of the canyon-channel. An, Angola; DRC, Democratic Republic of the Congo; RC, Republic of the Congo.

(Azpiroz-Zabala et al., 2017; Simmons et al., 2020). These ADCP-moorings survived relatively slow ($<2\text{--}3\text{ m s}^{-1}$) flows and showed that these turbidity currents comprised a faster-moving frontal zone (termed a “frontal-cell”) that outran a slower body (Azpiroz-Zabala et al., 2017).

A deployment of ADCP-moorings, along with the SAT-3 (South Atlantic 3) and WACS (West Africa Cable System) telecommunications cables, were broken by a canyon-flushing turbidity current in the Congo Canyon-Channel on 14–16 January 2020. Timings of these breaks documented flow front speeds of $5.0\text{--}8.2\text{ m s}^{-1}$ (Talling et al., 2022). The repaired SAT-3 cable was broken again on 8 March 2020 by another powerful flow. Talling et al. (2022) suggested these turbidity currents were preconditioned by major river floods with recurrence intervals of 20–50 years, and finally triggered by spring tides.

3. Materials and Methods

3.1. Instrument Deployment

Twelve OBSs and 11 moorings with ADCPs were deployed in September–October 2019 along the Congo Canyon-Channel, split into canyon and channel subarrays (Figure 1). The OBS instruments contained three-channel geophones (with a flat response $>5\text{ Hz}$) and hydrophones with sampling rates of 1 kHz. OBS1 to OBS8 contained Sercel L28-LB geophones and Hi-Tech HTI-90U hydrophones. The most distal OBS9 station contained an Owen (4.5 Hz) geophone and a Hi-Tech HTI-04 hydrophone, along with a thermometer logging temperature every minute. OBSs were deployed on the seafloor 0.7–2.9 km away from the center of the canyon-channel. In contrast, the 75, 300 and 600 kHz down-looking ADCP-moorings were suspended 44–250 m above the seafloor with anchors in the canyon-channel (Figures S1 and S2 in Supporting Information S1). The ADCP-moorings were broken by the January 2020 turbidity current (Talling et al., 2022). In contrast, the OBSs were not damaged by the canyon-flushing turbidity currents in January and March, and thus recorded the seismic signal of these events. Nine ADCPs and 10 OBS instruments were recovered.

3.2. OBS Data

Analysis focused on geophone data, as hydrophones on the OBSs did not record turbidity current signals. The vertical component of the geophone data were down-sampled to 100 Hz (Nyquist frequency of 50 Hz), as there were no relevant signals $>50\text{ Hz}$. The data was converted from raw counts to units of velocity and corrected to account for the instrument response (see Supporting Information S1). Next, spectrograms, illustrating signal power through time at different frequencies, were generated using a Fast Fourier Transform with a Hanning window of 20 s and a 50% overlap.

3.3. Identification and Quantification of Turbidity Currents in OBS and ADCP Data

Turbidity currents were visually identified from OBS spectrograms as distinct signals exhibiting a clear rise in seismic energy ($\sim 30\text{ dB}$ above background). These events typically show high-amplitude (up to $\sim 110\text{ dB}$) signals concentrated below 15 Hz, with a rapid onset over tens of seconds and gradual decay over hours. In the ADCP data, turbidity currents were identified as an abrupt increase in near-bed velocity of $>0.5\text{ m s}^{-1}$ (e.g., Azpiroz-Zabala et al., 2017).

Each event of enhanced seismic energy attributed to a turbidity current is termed a *pulse*, with turbidity currents comprising of one or more pulses. The turbidity current pulse runout distance is the location of the most distal OBS station that recorded a tracked pulse. The front transit speed of pulses (Table S1 in Supporting Information S1) was calculated by dividing the distance between OBS stations with the difference in pulse arrival times. Pulse duration was determined by manually picking the start and end of pulses from the seismic data (in counts) when the signal exceeded and then returned below 10% above background noise. The front-to-back length of pulses was estimated by multiplying the pulse transit velocity by pulse duration at each station (Table S1 in Supporting Information S1).

4. Results

Twenty pulses of seismic energy attributed to 16 separate turbidity currents were recorded by the OBS array during its 8-month deployment period (Figure S3 in Supporting Information S1).

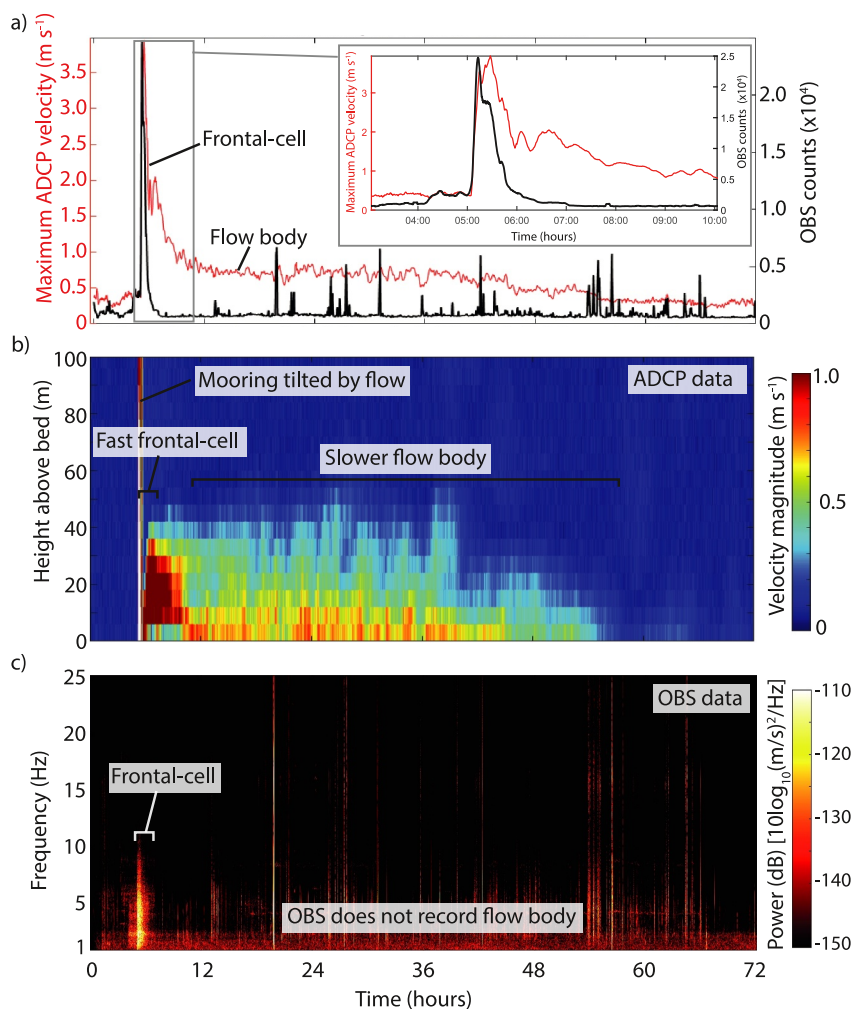


Figure 2. Comparison of acoustic Doppler current profiler (ADCP) and ocean-bottom seismograph (OBS) data for Flow 1. (a) Time series of ADCP maximum velocity for mooring M2 and corresponding seismic signal recorded by OBS3 (see Figure 1 for instrument locations). Inset shows zoom-in of flow front. (b) ADCP time series of turbidity current velocity profiles. (c) Spectrogram showing intensity of seismic signals during the turbidity current event.

4.1. Calibrating OBS Measurements Using ADCP Data

The ADCP-mooredings survived several relatively slow turbidity currents (Flows 1–9) before being broken by the first canyon-flushing event (Flow 10). ADCP velocity data can aid interpretation of the OBS seismic signals for weaker turbidity currents (Figure 2, Figures S4 and S5 in Supporting Information S1). For example, ADCP data show that Flow 1 contains a distinct, fast-moving ($\sim 4 \text{ m s}^{-1}$) frontal-cell (Azpiroz-Zabala et al., 2017), which lasts for ~ 2 hr (Figures 2a and 2b). Seismic data from the adjacent OBS registers the arrival of the flow with a rapidly emerging high-amplitude signal that corresponds to the turbidity current frontal-cell and lasts for ~ 30 min, before gradually decaying to background values over ~ 90 min (Figures 2a and 2c). The OBS does not record any signal from the flow body, yet the ADCP records a flow body lasting 2 days and traveling at 0.5 – 0.7 m s^{-1} .

OBSs recorded the fast ($> 1.6 \text{ m s}^{-1}$) frontal-cell's arrival ~ 4.5 – 37 min before the ADCP-mooredings. This suggests the turbidity current seismic signals are received from a straight-line distance of ~ 1.1 to 5.7 km away (see Supporting Information S1). There is no correlation between turbidity current maximum velocity and the estimated distance from which the OBS recorded the flow (Table S2 in Supporting Information S1). The hydrophones did not record any turbidity current acoustic signals (Figures S6 and S7 in Supporting Information S1), confirming that the geophones recorded ground-bound seismic signals generated by the turbidity currents.

Depth-averaged sediment concentrations derived from the ADCP-velocity measurements (via modified Chézy equations) demonstrate that the flow frontal-cells contained three-times higher depth-averaged sediment concentrations than the flow's body (Figure S8 in Supporting Information S1; Pope et al., 2022).

4.2. Seismic Characteristics of Short Runout Turbidity Currents

Most turbidity current pulses (16 of 20) terminated either within the canyon subarray (OBS1-4, runout distance <190 km) or before reaching the subarray of OBSs in the deep-water channel (OBS5-9, runout distance <791 km; Figures S3, S4, and S5 in Supporting Information S1). Transit velocities of these shorter flows ranged between 1.7 and 6.1 m s⁻¹, and their seismic pulse durations lasted 0.4–1.9 hr. The front-to-back length of these flow pulses varied between 4 and 32 km (Table S1 in Supporting Information S1).

4.3. Seismic Characteristics of Canyon-Flushing Turbidity Currents

The two canyon-flushing turbidity currents (Flows 10 and 11) traveled >1,000 km through the OBS array. Flow 10 contained three distinct seismic pulses (10A, 10B and 10C) over a period of 81 hr, demonstrating that a single turbidity current can be composed of discrete sub-events (Figure 3a). All pulses accelerated through the canyon subarray (Figure 3c), with pulse durations of 1.1–6.2 hr (Figure 3d). Pulse 10A and 10B amalgamated before reaching the deep-water channel to produce a single 13.4–14.7-hr pulse, with a maximum transit speed of 7.6 m s⁻¹ (Figure 3 and Figure S9 in Supporting Information S1). Pulse 10C reached a maximum transit speed of 6.4 m s⁻¹ in the channel with a duration of 4.6–6.6 hr. The pulses in Flow 10 are inferred to be part of one turbidity current; past work has recorded that turbidity currents can last for up to 10 days in the Congo Canyon (Simmons et al., 2020). Furthermore, temperature data from OBS9 (1,071 km offshore) recorded an increase in temperature that began with the arrival of the turbidity current and continued for ~21 days (Figure S10 in Supporting Information S1). This implies a continuous supply of warmer, shallow-sourced water via the turbidity current, which spilled out of the channel to reach the OBS station, ceasing as the turbidity current dissipated. Flow 11 comprised of a single pulse with speeds of 4.6–6.5 m s⁻¹ and durations of 2.1–4.8 hr in the canyon and channel (Figure 3 and Figure S9 in Supporting Information S1). For Flows 10 and 11, fast pulse transit speeds of >4.6 m s⁻¹ were either maintained or showed gradual deceleration in the 270-km-long channel subarray (Figure 3c). The front-to-back length of the seismic pulses were tens of kilometres long in the canyon and hundreds of kilometres long in the channel, with a maximum pulse length of ~400 km for Flow 10 (Figure 3d; Table S1 in Supporting Information S1).

5. Discussion

5.1. Internal Structure of Canyon-Flushing Turbidity Currents

Comparison of the seismic signal with ADCP-derived velocity data for short runout turbidity currents demonstrates that the seismic signals correspond to the flow frontal-cells (Figure 2), which have higher depth-averaged sediment concentrations than the flow body (Figure S8 in Supporting Information S1). Thus, we infer the seismic signals recorded for the canyon-flushing turbidity currents (Flows 10 and 11, where we lack ADCP data due to moorings breaking) are also produced by a fast and dense frontal-cell, albeit on a much greater scale, with durations 30 times longer than the weaker turbidity currents. Physical models have demonstrated the fast, coarse-grained, high-concentration part of debris flows generates the strongest seismic signals (Farin et al., 2019; Lai et al., 2018), supporting this interpretation.

5.2. Testing Models for Turbidity Current Flow Behavior

It has been widely inferred that seabed erosion by turbidity currents would increase their density, causing them to accelerate, leading to yet more erosion and further acceleration. This positive feedback was termed ignition (Figure 4a; Pantin, 1979; Parker, 1982; Parker et al., 1986). Talling et al. (2022) showed that the two canyon-flushing flows we observed eroded >1,300 Mt of sediment from the Congo Canyon-Channel. However, despite eroding a prodigious sediment mass, the seismic measurements reveal that the transit velocity of the frontal-cells of Flows 10 and 11 in the deep-water channel were near-uniform or gradually decelerating (Figure 3c). These transit velocity trends cannot be explained by changes in channel gradient or channel width, which are generally uniform (Hasenhüendl et al., 2024; Figure S11 in Supporting Information S1). Thus, the

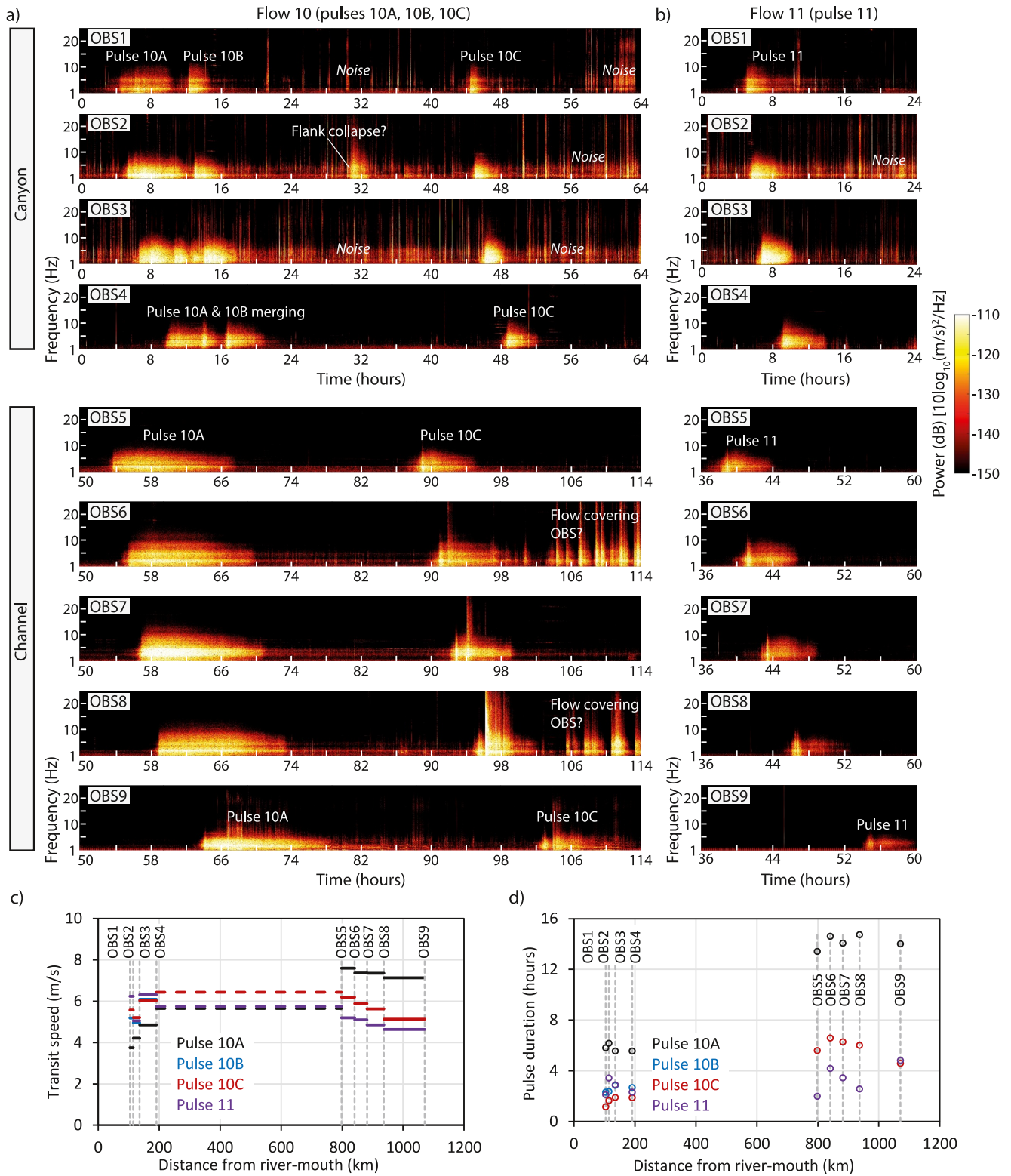


Figure 3. Seismic signals of Flows 10 and 11. (a, b) Spectrograms of seismic signal intensity with time recorded by ocean-bottom seismographs (OBSs) arranged in order of distance from the river-mouth (Figure 1). Flow 10 contained three pulses (10A, 10B and 10C), with pulses 10A and 10B amalgamating. Flow 11 comprises a single seismic pulse. For OBS6 and OBS8, signals continue after pulse 10C, possibly from the flow body overtopping the channel and covering the instruments. (c) Changes in pulse transit speed with distance. (d) Changes in pulse duration with distance.

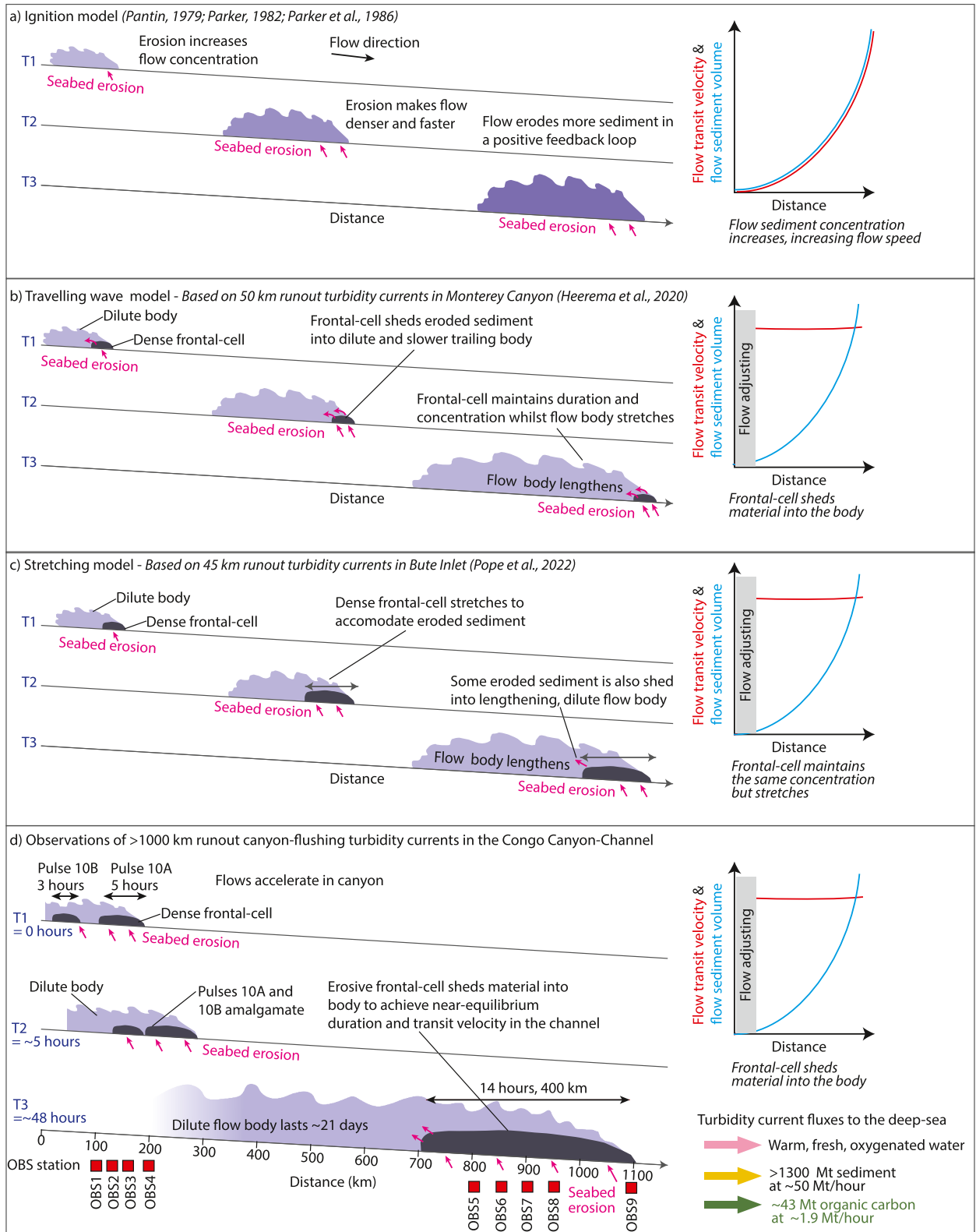


Figure 4.

erosive flows observed in the Congo Canyon-Channel require a process that maintains a near-uniform transit velocity despite extensive seabed erosion.

More recent flow models based on direct monitoring of short runout, shallow-water flows have included the presence of a dense frontal-cell and suggested processes by which erosive flows can maintain uniform transit speeds (Figures 4b and 4c; Heerema et al., 2020; Pope et al., 2022). The “traveling wave” model, established from observations of flows in Monterey Canyon, suggests flows maintain a near-uniform transit speed because entrainment of sediment into the leading part of the frontal-cell is balanced by deposition and shedding of sediment into a dilute trailing body (Figure 4b; Heerema et al., 2020; Paull et al., 2018). Measurements of flows in Bute Inlet led Pope et al. (2022) to propose that flow frontal-cells can bulk up via erosion, but instead of changing density, the frontal-cell stretches and thus a uniform flow velocity is maintained (Figure 4c). In both these models, the denser frontal-cell runs away from the dilute body, causing it to stretch (Azzipiroz-Zabala et al., 2017).

The OBS data document changes in the internal structure and duration of canyon-flushing turbidity currents for the first time, allowing flow models to be tested (Figure 4d). It is shown that canyon-flushing flows can comprise a series of pulses, and that pulses traveling at different speeds amalgamate (e.g., Pulses 10A & 10B). Once pulse-amalgamation is accounted for, however, only moderate changes in pulse-durations occur over long distances. For example, Pulse 10A shows little change in both front speed ($7.6\text{--}7.2\text{ m s}^{-1}$) and duration ($\sim 14\text{ hr}$) over 270 km in the deep-sea channel. Flow 11's seismic pulse shows modest variations in both its duration (2–5 hr) and front speed ($5.7\text{--}4.6\text{ m s}^{-1}$) for $\sim 1,000\text{ km}$. The frontal-cells of canyon-flushing flows therefore tend toward a near-equilibrium state characterized by near-uniform frontal speeds and durations. These observations are most consistent with the “traveling wave” model (Figure 4b) and suggest that only a small fraction of the eroded sediment is incorporated into a growing frontal-cell; most eroded sediment is shed backwards from the frontal-cell into the dilute trailing body (Figure 4d). Flow stretching is likely to occur in the flow body, as suggested by our observation that flows overspilled from the deep-sea channel for ~ 21 days.

5.3. Turbidity Current Fluxes to the Deep-Sea

Elevated water temperature measurements at OBS9 record overspill of Flow 10's body from the nearby channel, suggesting that Flow 10 lasted for ~ 21 days (Figure S10 in Supporting Information S1). Warmer water transferred $>1,000\text{ km}$ offshore by the turbidity currents is likely to have a higher oxygen content and lower salinity than the surrounding deep-water, ventilating the deep-ocean (Kao et al., 2010; Quadfasel et al., 1990; Sholkovitz & Soutar, 1975). The canyon-flushing flows were preconditioned by major Congo River floods with estimated recurrence intervals of 20–50 years (Talling et al., 2022). This work thus shows how major rivers are linked to the deep-sea, and that river floods may contribute to deep-water renewal and regional ocean mixing on a decadal scale, which may have unexplored impacts on global ocean dynamics (Kao et al., 2010).

The two canyon-flushing turbidity currents eroded and transported $43 \pm 15\text{ Mt}$ of terrestrial organic carbon (Baker, Hage, et al., 2024), with most of this seabed erosion likely occurring via the frontal-cells, which dominate turbidity current fluxes (Supporting Information S1; Pope et al., 2022). This study shows the combined duration of the two canyon-flushing flow frontal-cells was $\sim 23\text{-hr}$. This total duration can be combined with the eroded organic carbon mass to determine that the terrestrial organic carbon flux within these turbidity currents was $\sim 1.9\text{ Mt hr}^{-1}$. This *hourly* flux value is similar to the *annual* particulate organic carbon flux of the Congo River (2 Mt yr^{-1} ; Coynel et al., 2005). Over a period of less than 1 day, the canyon-flushing turbidity currents carried an amount of organic carbon to the deep-sea comparable to the estimated annual mass flux of terrestrial organic carbon buried in marine sediments globally ($40\text{--}80\text{ Mt yr}^{-1}$; Hilton & West, 2020). The global frequency of canyon-flushing turbidity currents is unknown. However, these seismic data reveal the duration and extreme

Figure 4. Summary of previous turbidity current flow models at consecutive snap-shots in time (T1, T2, T3), compared to observations of canyon-flushing turbidity currents in this study. Plots on the right show generalized changes in flow transit velocity and entire flow sediment volume. (a) Flow ignition model in which erosion increases sediment concentration and density, and thus velocity, leading to yet more erosion in a positive feedback loop. (b) Traveling wave model, where erosion at the dense frontal-cell front is balanced by deposition and shedding of sediment into a dilute trailing body, enabling the flow to maintain a uniform transit speed. (c) Stretching model, where the erosive frontal-cell stretches to accommodate the extra sediment, maintaining a consistent flow thickness, density difference, and frontal speed. (d) Observations of erosive, canyon-flushing turbidity currents in this study shows that flows tend toward a near-equilibrium state characterized by near-uniform transit speeds and frontal-cell durations and lengths. These observations support the “traveling wave” model where the frontal-cell sheds sediment into the body, which likely stretches.

organic carbon flux carried by canyon-flushing turbidity currents, and thus explains how these flows can transport organic carbon efficiently.

6. Conclusions

This study shows how passive seismic monitoring can revolutionize the monitoring of turbidity currents. In the Congo Canyon-Channel, we recorded the internal structure and duration of two powerful canyon-flushing flows that ran out for >1,000 km. These flows contained dense frontal-cells that emitted recordable seismic signals and were up to ~400 km in length. Despite extensive seabed erosion, these frontal-cells maintained consistent durations and speeds for hundreds of kilometres, efficiently transporting large fluxes of organic carbon, sediment, and warm water. Monitoring these flows globally will enable turbidity current fluxes to the deep-sea to be constrained.

Data Availability Statement

The raw ADCP data (Talling et al., 2024) and OBS seismic data (Baker, Talling, et al., 2024) used to record turbidity currents in this study are available via the British Oceanographic Data Centre (BODC) with no access conditions.

Acknowledgments

We thank the shipboard parties of RRS James Cook cruises JC187 and JC209 and NERC's Ocean-Bottom Instrumentation Facility (OBIF–Minshull et al., 2005). GEOMAR and Ifremer provided additional OBS and ADCP-moorings. We thank Angola Cables for organising permissions to work in Angolan waters. We are grateful to UK National Marine Facilities and crews of RV Thevenin, Thor Frigg, Maria Francesca for retrieving the ADCP-moorings, assisted by University of Hull and Durham University. We greatly appreciate the help of Tim Greenfield in analyzing the seismic data. This work was supported by National Environment Research Council Grants NE/R001952/1, NE/S010068/1, and NE/R015953/1. M.L. B and E.P were funded by Leverhulme Trust Early Career Fellowships ECF-2021-566 and ECF-2018-267. M.A.C was supported by the NERC COP26 Adaption and Resilience Programme and the International Cable Protection Committee. S.H was funded by the European Union's Horizon 2020 research and innovation programme under the Marie Skłodowska-Curie Grant 899546. M.J.B.C was funded by Royal Society Dorothy Hodgkin Fellowship DHFR1\180166.

References

- Arai, K., Naruse, H., Miura, R., Kawamura, K., Hino, R., Ito, Y., et al. (2013). Tsunami-generated turbidity current of the 2011 Tohoku-Oki earthquake. *Geology*, *41*(11), 1195–1198. <https://doi.org/10.1130/G34777.1>
- Azpiroz-Zabala, M., Cartigny, M. J. B., Talling, P. J., Parsons, D. R., Sumner, E. J., Clare, M. A., et al. (2017). Newly recognized turbidity current structure can explain prolonged flushing of submarine canyons. *Science Advances*, *3*(10). <https://doi.org/10.1126/sciadv.1700200>
- Babonneau, N., Savoye, B., Cremer, M., & Bez, M. (2010). Sedimentary architecture in meanders of a submarine channel: Detailed study of the present Congo Turbidite channel (Zaiango project). *Journal of Sedimentary Research*, *80*(10), 852–866. <https://doi.org/10.2110/jsr.2010.078>
- Baker, M. L., Hage, S., Talling, P. J., Acikalin, S., Hilton, R. G., Haghipour, N., et al. (2024a). Globally significant mass of terrestrial organic carbon efficiently transported by canyon-flushing turbidity currents. *Geology*, *52*(8), 631–636. <https://doi.org/10.1130/g51976.1>
- Baker, M. L., Talling, P. J., Peirce, C., & Pitcairn, B. (2024b). Ocean bottom seismograph data deployed along the Congo submarine canyon and channel (Atlantic Ocean) on cruise JC187, September 2019–September 2020. (Version 1) [Dataset]. *NERC EDS British Oceanographic Data Centre NOC*. <https://doi.org/10.5285/1D4A3BF0-FEAB-465C-E063-7086ABC0EF74>
- Carter, L., Milliman, J. D., Talling, P. J., Gavey, R., & Wynn, R. B. (2012). Near-synchronous and delayed initiation of long run-out submarine sediment flows from a record-breaking river flood, offshore Taiwan. *Geophysical Research Letters*, *39*(12), 6–10. <https://doi.org/10.1029/2012GL051172>
- Clare, M. A., Lintern, G., Pope, E., Baker, M., Ruffell, S., Zulkifli, M. Z., et al. (2024). Seismic and acoustic monitoring of submarine landslides. *Geophysical Monograph Series*, 59–82. <https://doi.org/10.1002/9781119750925.ch5>
- Cook, K. L., & Dietze, M. (2022). Seismic advances in process Geomorphology. *Annual Review of Earth and Planetary Sciences*, *50*(1), 183–204. <https://doi.org/10.1146/annurev-earth-032320-085133>
- Coyne, A., Seyler, P., Etcheber, H., Meybeck, M., & Orange, D. (2005). Spatial and seasonal dynamics of total suspended sediment and organic carbon species in the Congo River. *Global Biogeochemical Cycles*, *19*(4), 1–17. <https://doi.org/10.1029/2004GB002335>
- Fan, W., McGuire, J. J., & Shearer, P. M. (2020). Abundant spontaneous and dynamically triggered submarine landslides in the Gulf of Mexico. *Geophysical Research Letters*, *47*(12), 1–10. <https://doi.org/10.1029/2020GL087213>
- Farin, M., Tsai, V. C., Lamb, M. P., & Allstadt, K. E. (2019). A physical model of the high-frequency seismic signal generated by debris flows. *Earth Surface Processes and Landforms*, *44*(13), 2529–2543. <https://doi.org/10.1002/esp.4677>
- Galy, V., France-Lanord, C., Beyssac, O., Faure, P., Kudrass, H., & Palhol, F. (2007). Efficient organic carbon burial in the Bengal fan sustained by the Himalayan erosional system. *Nature*, *450*(7168), 407–410. <https://doi.org/10.1038/nature06273>
- Gavey, R., Carter, L., Liu, J. T., Talling, P. J., Hsu, R., Pope, E., & Evans, G. (2017). Frequent sediment density flows during 2006 to 2015, triggered by competing seismic and weather events: Observations from subsea cable breaks off southern Taiwan. *Marine Geology*, *384*, 147–158. <https://doi.org/10.1016/j.margeo.2016.06.001>
- Gomberg, J., Ariyoshi, K., Hautala, S., & Johnson, H. P. (2021). The finicky nature of earthquake shaking-triggered submarine sediment slope failures and sediment gravity flows. *Journal of Geophysical Research: Solid Earth*, *126*(10), 1–26. <https://doi.org/10.1029/2021jb022588>
- Hasenhündl, M., Talling, P. J., Pope, E. L., Baker, M. L., Heijnen, M. S., Ruffell, S. C., et al. (2024). Morphometric fingerprints and downslope evolution in bathymetric surveys: Insights into morphodynamics of the Congo canyon-channel. *Frontiers in Earth Science*, *12*(May), 1–19. <https://doi.org/10.3389/feart.2024.1381019>
- Heerema, C. J., Talling, P. J., Cartigny, M. J., Paull, C. K., Bailey, L., Simmons, S. M., et al. (2020). What determines the downstream evolution of turbidity currents? *Earth and Planetary Science Letters*, *532*, 116023. <https://doi.org/10.1016/j.epsl.2019.116023>
- Hilton, R. G., & West, A. J. (2020). Mountains, erosion and the carbon cycle. *Nature Reviews Earth & Environment*, *1*(6), 284–299. <https://doi.org/10.1038/s43017-020-0058-6>
- Kao, S. J., Dai, M., Selvaraj, K., Zhai, W., Cai, P., Chen, S. N., et al. (2010). Cyclone-driven Deep sea injection of freshwater and heat by Hyperpycnal flow in the subtropics. *Geophysical Research Letters*, *37*(21), 1–5. <https://doi.org/10.1029/2010GL044893>
- Khripounoff, A., Vangriesheim, A., Babonneau, N., Crassous, P., Dennielou, B., & Savoye, B. (2003). Direct observation of intense turbidity current activity in the Zaire submarine valley at 4000 m water depth. *Marine Geology*, *194*(3–4), 151–158. [https://doi.org/10.1016/S0025-3227\(02\)00677-1](https://doi.org/10.1016/S0025-3227(02)00677-1)
- Lai, V. H., Tsai, V. C., Lamb, M. P., Ulizio, T. P., & Beer, A. R. (2018). The seismic signature of debris flows: Flow mechanics and early warning at Montecito, California. *Geophysical Research Letters*, *45*(11), 5528–5535. <https://doi.org/10.1029/2018GL077683>

- Luckett, R., Baptie, B., Ottemoller, L., & Thompson, G. (2007). Seismic monitoring of the Soufrière Hills Volcano, Montserrat. *Seismological Research Letters*, 78(2), 192–200. <https://doi.org/10.1785/gssrl.78.2.192>
- Minshull, T. A., Sinha, M. C., & Peirce, C. (2005). Multi-disciplinary, sub-seabed geophysical imaging – A new pool of 28 seafloor instruments in use by the United Kingdom ocean bottom instrument Consortium. *Sea Technology*, 46(10), 27–31.
- Mountjoy, J. J., Howarth, J. D., Orpin, A. R., Barnes, P. M., Bowden, D. A., Rowden, A. A., et al. (2018). Earthquakes drive large-scale submarine canyon development and sediment supply to deep-ocean basins. *Science Advances*, 4(3). <https://doi.org/10.1126/sciadv.aar3748>
- Pantin, H. M. (1979). Interaction between velocity and effective density in turbidity flow: Phase-plane analysis, with criteria for autosuspension. *Marine Geology*, 31(1–2), 59–99. [https://doi.org/10.1016/0025-3227\(79\)90057-4](https://doi.org/10.1016/0025-3227(79)90057-4)
- Parker, G. (1982). Conditions for the ignition of catastrophically erosive turbidity currents. *Marine Geology*, 46(3–4), 307–327. [https://doi.org/10.1016/0025-3227\(82\)90086-X](https://doi.org/10.1016/0025-3227(82)90086-X)
- Parker, G., Fukushima, Y., & Pantin, H. M. (1986). Self-accelerating turbidity currents. *Journal of Fluid Mechanics*, 171(1), 145. <https://doi.org/10.1017/S0022112086001404>
- Paull, C. K., Talling, P. J., Maier, K. L., Parsons, D., Xu, J., Caress, D. W., et al. (2018). Powerful turbidity currents driven by dense basal layers. *Nature Communications*, 9(1), 1–9. <https://doi.org/10.1038/s41467-018-06254-6>
- Pope, E. L., Cartigny, M. J. B., Clare, M. A., Talling, P. J., Lintern, D. G., Vellinga, A., et al. (2022). First source-to-sink monitoring shows dense head controls sediment flux and runoff in turbidity currents. *Science Advances*, 8(20). <https://doi.org/10.1126/sciadv.abj3220>
- Pope, E. L., Talling, P. J., Carter, L., Clare, M. A., & Hunt, J. E. (2017). Damaging sediment density flows triggered by tropical cyclones. *Earth and Planetary Science Letters*, 458, 161–169. <https://doi.org/10.1016/j.epsl.2016.10.046>
- Quadfasel, D., Kudrass, H., & Frische, A. (1990). Deep-water renewal by turbidity currents in the Sulu Sea. *Nature*, 348(6299), 320–322. <https://doi.org/10.1038/348320a0>
- Savoie, B., Babonneau, N., Dennielou, B., & Bez, M. (2009). Geological overview of the Angola-Congo margin, the Congo deep-sea fan and its submarine valleys. *Deep-Sea Research Part II Topical Studies in Oceanography*, 56(23), 2169–2182. <https://doi.org/10.1016/j.dsr2.2009.04.001>
- Seabrook, S., Mackay, K., Watson, S. J., Clare, M. A., Hunt, J. E., Yeo, I. A., et al. (2023). Volcaniclastic density currents explain widespread and diverse seafloor impacts of the 2022 Hunga Volcano eruption. *Nature Communications*, 14(1), 7881. <https://doi.org/10.1038/s41467-023-43607-2>
- Sen, A., Dennielou, B., Tourolle, J., Arnaubec, A., Rabouille, C., & Olu, K. (2017). Fauna and habitat types driven by turbidity currents in the lobe complex of the Congo deep-sea fan. *Deep-Sea Research Part II Topical Studies in Oceanography*, 142(May), 167–179. <https://doi.org/10.1016/j.dsr2.2017.05.009>
- Sgroi, T., Monna, S., Embriaco, D., Giovanetti, G., Marinaro, G., & Favali, P. (2014). Geohazards in the Western Ionian Sea: Insights from non-earthquake signals recorded by the Nemo-Sn1 seafloor observatory. *Oceanography*, 27(2), 154–166. <https://doi.org/10.5670/oceanog.2014.51>
- Sholkovitz, E., & Soutar, A. (1975). Changes in the composition of the bottom water of the Santa Barbara basin: Effect of turbidity currents. *Deep-Sea Research and Oceanographic Abstracts*, 22(1), 13–21. [https://doi.org/10.1016/0011-7471\(75\)90014-5](https://doi.org/10.1016/0011-7471(75)90014-5)
- Shugar, D. H., Jacquemart, M., Shean, D., Bhushan, S., Upadhyay, K., Sattar, A., et al. (2021). A massive rock and ice avalanche caused the 2021 disaster at Chamoli, Indian Himalaya. *Science*, 373(6552), 300–306. <https://doi.org/10.1126/science.abh4455>
- Simmons, S. M., Azpiroz-Zabala, M., Cartigny, M. J. B., Clare, M. A., Cooper, C., Parsons, D. R., et al. (2020). Novel acoustic method provides first detailed measurements of sediment concentration structure within submarine turbidity currents. *Journal of Geophysical Research: Oceans*, 125(5), 1–24. <https://doi.org/10.1029/2019jc015904>
- Talling, P. J., Baker, M. L., Pope, E. L., Ruffell, S. C., Jacinto, R. S., Heijnen, M. S., et al. (2022). Longest sediment flows yet measured show how major rivers connect efficiently to deep sea. *Nature Communications*, 13(1), 1–15. <https://doi.org/10.1038/s41467-022-31689-3>
- Talling, P. J., Baker, M. L., Simmons, S. M., Pope, E. L., Ruffell, S., & Silva Jacinto, R. (2024). Downward looking Acoustic Doppler Current Profiler (ADCP) data from moorings deployed along the Congo submarine canyon and channel (Atlantic ocean) deployed on cruise JC187, September 2019–January 2020. (Version 1) [Dataset]. *NERC EDS British Oceanographic Data Centre NOC*. <https://doi.org/10.5285/246E4380-DECO-80BF-E063-7086ABC049DA>
- Talling, P. J., Cartigny, M. J. B., Pope, E., Baker, M., Clare, M. A., Heijnen, M., et al. (2023). Detailed monitoring reveals the nature of submarine turbidity currents. *Nature Reviews Earth & Environment*, 4(9), 642–658. <https://doi.org/10.1038/s43017-023-00458-1>
- Vangriesheim, A., Khrpounoff, A., & Crassous, P. (2009). Turbidity events observed in situ along the Congo submarine channel. *Deep-Sea Research Part II Topical Studies in Oceanography*, 56(23), 2208–2222. <https://doi.org/10.1016/j.dsr2.2009.04.004>

References From the Supporting Information

- Burtin, A., Hovius, N., & Turowski, J. M. (2016). Seismic monitoring of torrential and fluvial processes. *Earth Surface Dynamics*, 4(2), 285–307. <https://doi.org/10.5194/esurf-4-285-2016>
- Beyreuther, M., Barsch, R., Krischer, L., Megies, T., Behr, Y., & Wassermann, J. (2010). ObsPy: A Python toolbox for seismology. *Seismological Research Letters*, 81(3), 530–533. <https://doi.org/10.1785/gssrl.81.3.530>
- Parker, G., Garcia, M., Fukushima, Y., & Yu, W. (1987). Experiments on turbidity currents over an erodible bed. *Journal of Hydraulic Research*, 25(1), 123–147. <https://doi.org/10.1080/00221688709499292>
- Ruffell, S. C., Talling, P. J., Baker, M. L., Pope, E. L., Heijnen, M. S., Jacinto, R. S., et al. (2024). Time-lapse surveys reveal patterns and processes of erosion by exceptionally powerful turbidity currents that flush submarine canyons: A case study of the Congo canyon. *Geomorphology*, 463, 109350. <https://doi.org/10.1016/j.geomorph.2024.109350>